

Optic disc and cup segmentation in fundus retinal images using feature detection and morphological techniques

R. Priyadharsini^{1,*}, A. Beulah¹ and T. Sree Sharmila²

¹Department of Computer Science and Engineering, and

²Department of Information Technology, SSN College of Engineering, Kalavakkam 603 110, India

Segmentation of optic disc and cup from the fundus retinal image helps in the detection of glaucoma which is one of the important causes for vision loss. In this study, we propose a method for optic disc followed by optical cup segmentation. The retinal input image is first preprocessed by applying histogram equalization and the connected components in the image are obtained. On applying the circle detection Hough transform, the circular-shaped optic disc is segmented from the other connected components. The morphological closing operation is applied on the segmented optic disc area to identify the optic cup location. The optic cup is then segmented by applying Otsu's thresholding only on the extracted green channel of the retinal image. The proposed method was evaluated using DRISHTI-GS dataset containing 50 test images. The performance metrics such as dice coefficient, average boundary localization error and cup–disc ratio error were obtained by comparing the proposed method with the ground truth values of 51 training images in the DRISHTI-GS dataset.

Keywords: Feature detection, fundus retinal image, morphological closing, optic disc and cup, segmentation.

THE state-of-the-art segmentation techniques in digital image processing tend to detect objects in the images. These segmentation methods identify the objects by extracting features such as colour, edges, interest points, ridges, etc. When the features are more dominant in the images, the segmentation methods successfully identify the objects. The real challenge of these techniques is when the features of foreground, background and region of interest (ROI) are not differentiable from the image. The retinal fundus image is one such example where the ROI cannot be segmented clearly by the traditional segmentation methods. Eyes are among the most important organs of the human body, which should be monitored constantly. There are many modalities such as fundus photography, autofluorescence, infrared reflectance, etc. for capturing the fundus images¹. They help in detection and further prevention of eye-related diseases like diabetic retinopathy, hypertensive retinopathy, age-related macular degeneration, glaucoma, leukaemia, etc. The main components of the retina are blood vessels,

optic disc and optic cup. Figure 1 shows the sample fundus images taken from the training images of DRISHTI-GS dataset. It is clear from the figure that the dataset contains fundus images with different contrast and brightness. The blood vessels, disc and cup merge in the image, making the feature extraction more demanding. Determining the cup–disc ratio (CDR) is essential for detecting the disease for which segmentation of disc and cup from the retinal images is necessary. In this study, we propose two different methods for optic disc and cup segmentation.

The conventional segmentation methods such as edge-based, region-based and morphological-based segmentation are generally used for object detection and for extracting meaningful information from the image for analysis². The characteristics of the fundus images are unique, where the features of the ROI are not dominant. Many methods have been proposed for optic disc and cup segmentation with standard datasets such as STARE, DRIVE, MESSIDOR, DIARETDB1, CHASE_DB1, DRIONS-DB, etc. Table 1 shows the related studies with methods, datasets and number of images used for optic disc and cup segmentation^{3–13}. In the literature, various optic disc and cup segmentation methodologies for glaucoma image detection have been analysed¹⁴.

The optic disc is a circular, yellowish region that appears to be the brightest area in the fundus image. The yellowish colour is due to the absence of pigmented epithelium in this zone. The objective of this study is to first segment the disk. The test images from DRISHTI-GS dataset are considered as input for the proposed method. The red (R), green (G) and blue (B) planes are extracted and enhanced using histogram equalization. The overall distance (D) from the given colour image is calculated and a mask is created using the obtained distance. The distances D_R , D_G , D_B in the R, G and B planes are obtained by the difference of each plane with the threshold T . The overall distance D is calculated as the sum of the squares of the distances D_R , D_G and D_B . The distance image contains optic disc and blood vessels. Due to the indistinguishable boundaries, presence of capillaries and other structures in the neighbourhood of the optic disc region, localization of the area is a difficult task. Therefore, a mask (M) is created by eliminating all the darker pixels which removes most of the blood vessels and retains the optic disc. The obtained mask still contains tissues whose pixel values are more similar to that of the optic disc. So, in the mask image, all the connected components (CCs) are identified. The centre points for all the connected components are obtained and the optic disk which is the ROI is

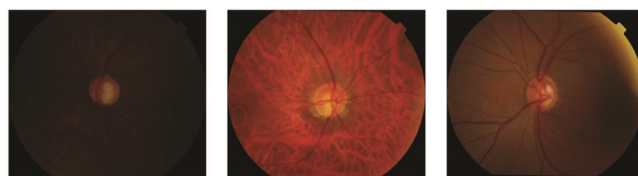


Figure 1. Sample training images from DRISHTI-GS dataset.

*For correspondence. (e-mail: priyadharsinir@ssn.edu.in)

Table 1. Literature survey on optic disk and cup segmentation

| Reference | Method used | Dataset | Number of images used |
|--------------------------------------|---|--|-----------------------|
| Youssif <i>et al.</i> ³ | Vessels' direction matched filter | STARE DRIVE | 81 40 |
| Aquino <i>et al.</i> ⁴ | Morphological, edge detection, and feature extraction techniques | MESSIDOR | 1200 |
| Welfer <i>et al.</i> ⁵ | Adaptive morphological approach | DRIVE DIARETDB1 | 40 89 |
| Abdullah <i>et al.</i> ⁶ | Circular Hough transform and grow-cut algorithm | DRIVE, DIARETDB1, CHASE_DB1, DRIONS-DB, MESSIDOR and one local Shifa Hospital Database | |
| Dehghani <i>et al.</i> ⁷ | Histogram matching | DRIVE, STARE, and a local dataset | 273 |
| Ingle and Mishra ⁸ | Gradient method | Random images from different source | |
| Muramatsu <i>et al.</i> ⁹ | Active contour method, depth map on the basis of stereo disparity | Stereo retinal fundus images | 80 |
| Yin <i>et al.</i> ¹⁰ | Combines knowledge-based circular Hough transform and a novel optimal channel selection | ORIGA | 325 |
| Li and Chutatape ¹¹ | Modified active shape model | Obtained from clinics by topcon retinal camera | 35 |
| Cheng <i>et al.</i> ¹² | Superpixel classification by histograms and centre surround statistics | MESSIDOR | 650 |
| Tan <i>et al.</i> ¹³ | Multi-scale superpixel classification | ORIGA | 650 |

detected by eliminating the unwanted components. As the optic disk in the retina is a circular object, circle detection Hough transform is used for detecting the area. The centre point of the connected components which is close to the centre of the circle detected by the Hough transform is selected as the centre point of the optic disc. The circular object among the connected components is referred to as (CO).

Circle Hough transform (CHT) is an efficient technique to detect circles in the image². Shapes can be described in parametric form and a voting scheme is used to find the correct parameters. CHT relies on the equation of circles as follows

$$r^2 = (x - a)^2 + (y - b)^2, \quad (1)$$

where a and b are the coordinates for the centre of the circle, r the radius of the circle, and (x, y) are the pixel coordinates.

CHT uses the three-dimensional accumulator space for detecting circles with three parameters defined using eq. (2) below. All the edge points in the image are mapped to a set of circles in the accumulator space. The set of circles is defined by all possible values of the radius and centred on the coordinates of the edge point. The radius value remains constant and each edge point defines circles for the other values of the fixed radius. These edge points map to the cone of votes in the accumulator space. Using voting method, circles are detected using the maximum number of votes in the accumulator space which corresponds to the parameters of the circle. The parametric representation of the circle is given by

$$x = a + r \cos(\theta), \quad y = b + r \sin(\theta). \quad (2)$$

CHT is used for detecting the circular objects in the image. The corresponding connected component selected with the centre point forms the original optic disc. The boundary positions and area of the optic disc are obtained. A bounding box (BB) is estimated for the segmented optic disc. The region of interest which is the optic disc is cropped from the original image for further optic cup segmentation. Box 1 shows an algorithm with the steps involved in optic disc segmentation.

The optic cup present inside the disc region is not always circular in shape. After segmenting the optic disc, different methods should be followed to segment the optic cup. The shape of the cup varies with the eye and with glaucoma. Morphological closing operation is performed on the image to segment the optic cup. Closing operation smoothens the boundary areas by fusing narrow breaks, eliminates small holes and fills the gaps in the boundary. The closing operation (\bullet) is defined as

$$I \bullet S = (I \oplus S) \ominus S, \quad (3)$$

where I represents the input image and S is the circular structuring element. Based on the shape of the object to be detected in the image, the structuring element can be defined. The structuring element probes an image using hit or fit operations. In eq. (3), \oplus denotes the morphological dilation and \ominus denotes the morphological erosion. Dilation operation is used for thickening the boundaries of the objects of interest in the image, whereas erosion is used to shrink the boundaries. The extent of thickening and thinning is a function of shape of the structuring element used.

Box 1. Optic disc segmentation – algorithm

Input: Test images from *DRISHTI_GS* dataset

Output: Segmented optic disc from test image

Procedure:

1. Input a test image from the DRISHTI_GS dataset
2. Extract red, green, blue (**RGB**) channels for the given image
3. Apply histogram equalization for all the channels to enhance the contrast
4. Create a mask image (**M**) by calculating the overall distance from the extracted RGB channels
5. Obtain all the connected components (**CC**) from **M**.
6. Detect all the circular objects among the connected components (**CO**) by circle detection Hough transform
7. For all the **CC_i** in **M**

For all the **CO_i** in **M**

if ($\text{centroid}(\text{CC}_i) == \text{centroid}(\text{CO}_i)$)

opticaldisc_center = $\text{centroid}(\text{CC}_i)$;

opticaldisc_area = $\text{area}(\text{CO}_i)$;

estimate the bounding box (**BB**) for **CC_i** to be used for cup segmentation

else

eliminate the **CC_i** from **M**;

Box 2. Optic cup segmentation – algorithm

Input: Test images with bounding box **BB**

Output: Segmented optic cup

Procedure:

1. Create a disk-shaped structuring element (**SE**) with radius 10
2. Obtain a resultant image by executing morphological closing operation using **SE** on **BB**
3. Extract green channel from the resultant image
4. Perform Otsu’s thresholding on the green channel to obtain the optic cup

The morphological dilation and erosion are defined as follows in eqs (4) and (5) respectively

$$I \oplus S = \{z \mid (\hat{S})_z \cap I \neq \phi\}, \tag{4}$$

$$I \ominus S = \{z \mid (S)_z \subseteq I\}, \tag{5}$$

where *S* is the set of pixels representing an structuring element to be used to convolve over the object in an image. $(S)_z$ denotes translation of a set *S* by point *z* with (z_1, z_2) whose (x, y) coordinates have been replaced by $(x + z_1, y + z_2)$. (\hat{S}) denotes reflection on a set *S* whose (x, y) coordinates are replaced by $(-x, -y)$.

Dilation is based on the statistical property of reflection. The dilation of *I* by *S* is the set of all displacements *z* such that (\hat{S}) and *I* overlap by at least one element. Thus, dilation thickens the objects in a binary image. ϕ is the empty set. Erosion is based on translation property. The erosion of *I* by *S* is the set of all points *z*, such that *S* translated by *z* is contained in *I*. Thus, erosion shrinks the objects in a binary image. The origin of *S* would cause the structuring element to cease being completely contained in *I*.

Optic disc segmented from the original image is processed by morphological dilation followed by erosion operation using a circular structuring element. The green

channel is separated from the morphologically altered image. The Otsu’s thresholding method is applied on the green channel, which yields the optic cup. The boundary positions and area of the optic cup are obtained. Box 2 shows an algorithm with the steps involved in optic cup segmentation.

This work was implemented in MATLAB R2014a (ref. 15) on DRISHTI-GS dataset¹⁶. Figure 2 *a* shows test images from the dataset. Figure 2 *b* and *c* shows soft map of the optic disk and cup respectively. Figure 2 *d* shows the segmented optic disk and cup. In Figure 2 *d* the green colour boundary is the optic disc boundary and the blue colour boundary is the optic cup boundary.

The proposed method has been evaluated on DRISHTI-GS. Table 2 provides a summary of the dataset.

Dice similarity coefficient (DICE): This measures the extent of overlapping regions between any two images¹⁷. It does a comparison between ground truth and automated segmentation images. The ground truth segmented image is represented as S_g . The segmented test image is represented as S_t . In general, the segmented images are partitioned into two different classes¹⁸: the segmented anatomy as class 1 and background as class 2. Therefore, the anatomy in ground truth is represented as S_g^1 and the background in ground truth is denoted by S_g^2 . Similarly, the anatomy and background in the test images are represented as S_t^1 and S_t^2

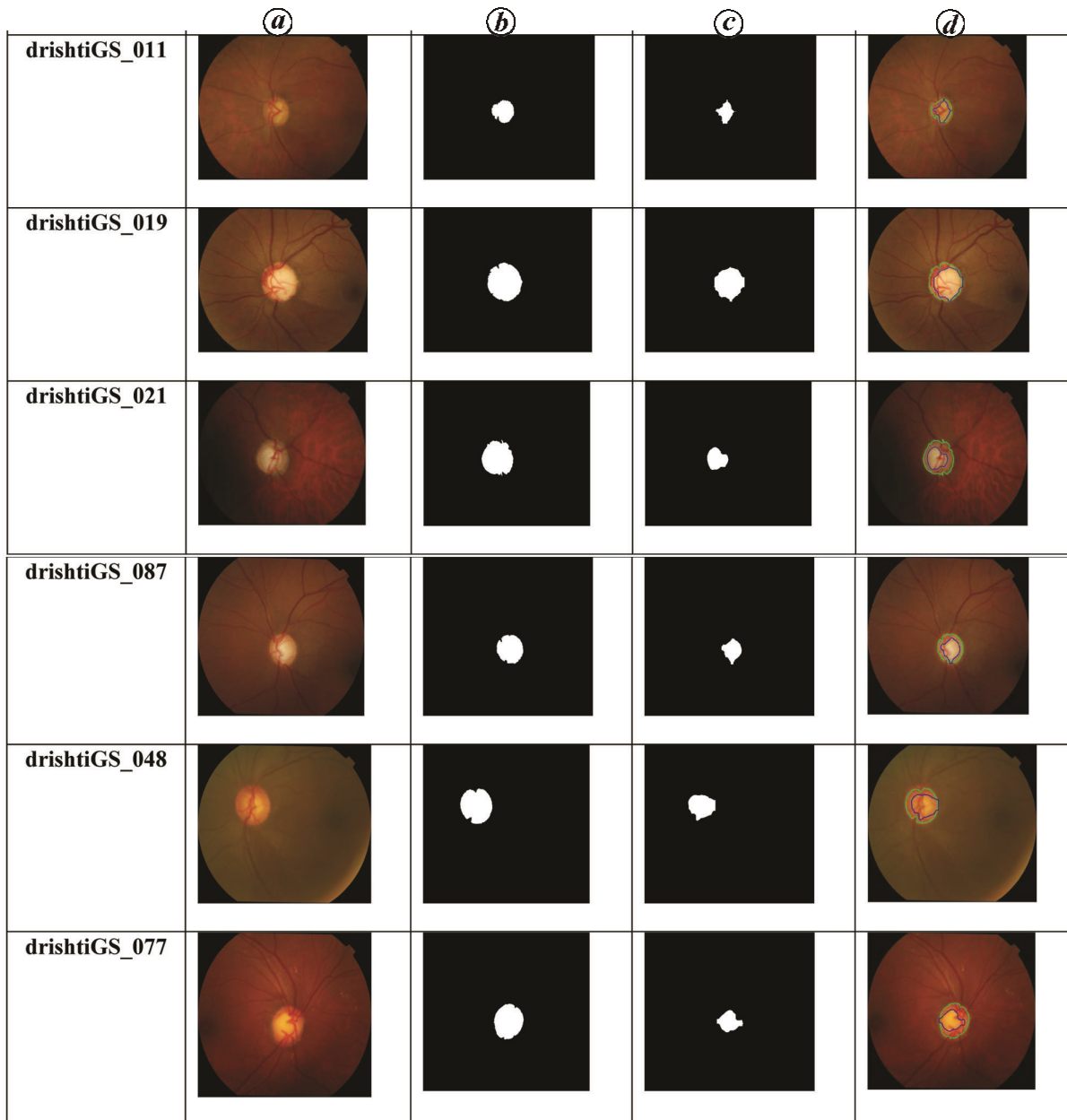


Figure 2. *a*, Test images from DRISHTI-GS dataset. *b*, Soft map of optic disc. *c*, Soft map of optic cup. *d*, Segmented optic disc and cup.

Table 2. Dataset specification

| | |
|--------------|--|
| Dataset | DRISHTI-GS |
| Images | 50 training, 51 testing images |
| Resolution | 2896 × 1944 |
| Ground truth | Softmap of optic disc and optic cup for training image |

respectively. Class 2 is omitted as it has only the background. DICE is defined as

$$DICE = \frac{2|S_g^1 \cap S_t^1|}{|S_g^1| + |S_t^1|} \tag{6}$$

Boundary distance localization error (BLE): As DICE does not provide the boundary-level performance analysis, BLE analysis is performed. BLE is the distance (in pixels) between the ground truth S_g^1 and test image S_t^1 boundaries. BLE is defined as

$$BLE = \frac{1}{n} \sum_{i=1}^n |r_i^g - r_i^t|, \tag{7}$$

where $|r_i^g - r_i^t|$ is Euclidean distance between the estimated boundary in S_t^1 and the centre of the ground truth in S_g^1 , in the i direction. n is the equi-spaced points.

Table 3. Performance measure on the DRISTHI-GS test images

| Optic disc | | Optic cup | |
|------------|-------------|-----------|-------------|
| DICE | BLE | DICE | BLE |
| 0.85/0.16 | 27.56/30.55 | 0.71/0.18 | 37.08/20.27 |

Cup-to-disc ratio: This is computed as the ratio of the vertical cup diameter to vertical disc diameter and accurate segmentation of cup and disc is essential for CDR measurement. CDR is calculated using the following formula

$$CDR = \frac{\text{Cup area}}{\text{Disc area}} \quad (8)$$

The CDR error is obtained by eq. (9)

$$CDR_{\text{error}} = |CDR_{\text{GT}} - CDR_{\text{Proposed}}| \quad (9)$$

Table 3 shows the performance measure on the test images. The absolute CDR error for the test images is 0.27/0.18.

All the 51 test images were tested using the proposed optic disc and cup segmentation method. All the test images are of varying brightness and contrast. The optic disc segmentation is done by first extracting the R, G and B planes and a mask image is created from the overall distance calculated. The optic disc is detected from the mask by CHT. All the other connected components are eliminated from the circular objects. The centre point of the connected components which is close to the centre of the circle detected by the Hough transform is selected as the centre point of the optic disc. The optic cup is segmented by applying the morphological closing operation. The green channel is separated from the morphologically altered image. The Otsu's thresholding method is applied on the green channel, which yields the optic cup. The boundary positions and area of the optic cup are obtained. Among the images, 88% of the test images works well for the proposed method. When compared to the ground truth values given in the dataset, absolute CDR error obtained is 0.27.

- Welfer, D., Scharcanski, J., Kitamura, C. M., Dal Pizzol, M. M., Ludwig, L. W. and Marinho, D. R., Segmentation of the optic disk in color eye fundus images using an adaptive morphological approach. *Comput. Biol. Med.*, 2010, **40**(2), 124–137.
- Abdullah, M., Fraz, M. M. and Barman, S. A., Localization and segmentation of optic disc in retinal images using circular Hough transform and grow-cut algorithm. *Peer J*, 2016, **4**, e2003.
- Dehghani, A., Moghaddam, H. A. and Moin, M. S., Optic disc localization in retinal images using histogram matching. *EURASIP J. Image Video Process.*, 2012, **2012**, 11, 19.
- Ingle, R. and Mishra, P., Cup segmentation by gradient method for the assessment of glaucoma from retinal image. *Int. J. Eng. Trends Technol.*, 2013, **4**(6), 2540–2543.
- Muramatsu, C., Nakagawa, T., Sawada, A., Hatanaka, Y., Yamamoto, T. and Fujita, H., Automated determination of cup-to-disc ratio for classification of glaucomatous and normal eyes on stereo retinal fundus images. *J. Biomed. Opt.*, 2011, **16**(9), 096009-1–096009-7.
- Yin, F., Liu, J., Wong, D. W. K., Tan, N. M., Cheung, C., Baskaran, M. and Wong, T. Y., Automated segmentation of optic disc and optic cup in fundus images for glaucoma diagnosis. In 25th IEEE International Symposium on Computer-based Medical Systems, 2012, pp. 1–6.
- Li, H. and Chutatape, O., Boundary detection of optic disk by a modified ASM method. *Pattern Recogn.*, 2003, **36**(9), 2093–2104.
- Cheng, J. *et al.*, Superpixel classification based optic disc and optic cup segmentation for glaucoma screening. *IEEE Trans. Med. Imaging*, 2013, **32**(6), 1019–1032.
- Tan, N. M., Xu, Y., Goh, W. B. and Liu, J., Robust multi-scale superpixel classification for optic cup localization. *Comput. Med. Imaging Graphics*, 2015, **40**, 182–193.
- Almazroa, A. *et al.*, Optic disc and optic cup segmentation methodologies for glaucoma image detection: a survey. *J. Ophthalmol.*, 2015, 180972-1–180972-28.
- Mathworks, I., MATLAB: R2014a. Mathworks Inc, Natick, MA, USA, 2014.
- Sivaswamy, J., Krishnadas, S. R., Joshi, G. D., Jain, M. and Tabish, A. U. S., DRISHTI-GS: retinal image dataset for optic nerve head (onh) segmentation. In 11th IEEE International Symposium on Biomedical Imaging, April 2014, pp. 53–56.
- Dice, L. R., Measures of the amount of ecologic association between species. *Ecology*, 1945, **26**(3), 297–302.
- Taha, A. A. and Hanbury, A., Metrics for evaluating 3D medical image segmentation: analysis, selection, and tool. *BMC Med. Imaging*, 2015, **15**(1), 29.

Received 9 November 2017; revised accepted 13 May 2018

doi: 10.18520/cs/v115/i4/748-752

- Jain, A. B., Prakash, V. J. and Bhende, M., Techniques of fundus imaging. *Med. Vis. Res. Foundations*, 2015, **33**(2), 100.
- Gonzalez, R. C. and Woods, R. E., Image processing. In *Digital Image Processing*, Prentice Hall, New Jersey, USA, 2007, pp. 104–168.
- Youssif, Aliaa Abdel-Haleim Abdel-Razik, Atef Zaki Ghalwash, and Amr Ahmed Sabry Abdel-Rahman Ghoneim, Optic disc detection from normalized digital fundus images by means of a vessels' direction matched filter. *IEEE Trans. Med. Imaging*, 2008, **27**(1), 11–18.
- Aquino, A., Gegúndez-Arias, M. E. and Marín, D., Detecting the optic disc boundary in digital fundus images using morphological, edge detection, and feature extraction techniques. *IEEE Trans. Med. Imaging*, 2010, **29**(11), 1860–1869.